# Alterations in Hippocampal Network Activity after *In Vitro* Traumatic Brain Injury

Woo Hyeun Kang,[1] Wenzhe Cao,[2] Oliver Graudejus,[2,3] Tapan P. Patel,[4] Sigurd Wagner,[2]
David F. Meaney,[4] and Barclay Morrison, III[1]

## Abstract

Traumatic brain injury (TBI) alters function and behavior, which can be characterized by changes in electrophysiological function *in vitro*. A common cognitive deficit after mild-to-moderate TBI is disruption of persistent working memory, of which the *in vitro* correlate is long-lasting, neuronal network synchronization that can be induced pharmacologically by the gamma-aminobutyric acid A antagonist, bicuculline. We utilized a novel *in vitro* platform for TBI research, the stretchable microelectrode array (SMEA), to investigate the effects of TBI on bicuculline-induced, long-lasting network synchronization in the hippocampus. Mechanical stimulation significantly disrupted bicuculline-induced, long-lasting network synchronization 24 h after injury, despite the continued ability of the injured neurons to fire, as revealed by a significant increase in the normalized spontaneous event rate in the dentate gyrus (DG) and CA1. A second challenge with bicuculline 24 h after the first challenge significantly decreased the normalized spontaneous event rate in the DG. In addition, we illustrate the utility of the SMEA for TBI research by combining multiple experimental paradigms in one platform, which has the potential to enable novel investigations into the mechanisms responsible for functional consequences of TBI and speed the rate of drug discovery.

**Key words:** electrophysiology; hippocampus; network synchronization; traumatic brain injury

## Introduction

**T**RAUMATIC BRAIN INJURY (TBI) continues to be a leading cause of death and disability,[1,2] affecting nearly 10 million people annually worldwide and an estimated 1.7 million people annually in the United States.[3] The devastating behavioral and functional consequences of TBI include cognitive impairment,[4] memory loss or impairment,[5] loss or decreased consciousness,[6] motor deficits,[7] coma,[8] seizure and epilepsy,[9] and death.[10]

Disruption of persistent working memory is a prominent cognitive deficit experienced by individuals with TBI.[11] In adults, the neural correlate for working memory and information storage may be recurrent network activity,[12] which is also involved in neuronal network maturation in the developing brain.[13] In many cases, working memory deficits arise in the absence of cell death or overt structural damage to brain tissue, especially in cases of mild or moderate TBI.[14–17]

TBI is caused by deformation of brain tissue, with tissue strain and strain rate identified as significant predictors of injury.[18–21] However, very few studies have characterized *in vivo* tissue strain and strain rate during TBI owing to the challenges of directly measuring tissue deformation *in vivo*.[22–24] An *in vitro* approach to these mechanistic studies allows for precise control of the mechanical stimulus and the extracellular environment to examine the response of the brain parenchyma in the absence of systemic influences, while recapitulating much of the *in vivo* pathology.[25,26]

One way to record *in vitro* neural activity is through the use of microelectrode arrays (MEAs).[17,27,28] Compared to single-electrode electrophysiological recordings, MEAs enable the investigation of higher order behaviors of neuronal networks comprised of up to many thousands of neurons, owing to the ability to record simultaneously from multiple sites.[29,30] One limitation of available MEAs is their rigid nature, which prevents direct testing of hypotheses relating changes in electrophysiological function to mechanisms of mechanotransduction. Previously, we demonstrated the ability to monitor electrophysiological function in hippocampal slice cultures after mechanical stretch injury using an earlier generation of SMEAs (stretchable microelectrode arrays).[31] In the present study, we leveraged the advantages of the latest generation of SMEA, with more recording electrodes and smaller feature size, to test our hypothesis that long-lasting, hippocampal network synchronization is disrupted by TBI.

[1]Department of Biomedical Engineering, Columbia University, New York, New York.
[2]Department of Electrical Engineering, Princeton University, Princeton, New Jersey.
[3]Department of Chemistry and Biochemistry, Arizona State University, Tempe, Arizona.
[4]Department of Bioengineering, University of Pennsylvania, Philadelphia, Pennsylvania.

Recurrent network activity or synchronization is regulated by the inhibitory neurotransmitter, gamma-aminobutyric acid (GABA).[32] Disinhibition, caused by disruptions in GABAergic signaling, may be a leading cause of pathologically persistent activity.[33] Acutely, the $GABA_A$ antagonist, bicuculline, is used to induce epileptiform bursting activity in brain slice cultures by blocking GABAergic inhibition[34] and to induce long-lasting, recurrent synchronous bursting, hours and days after washout.[28,35] By utilizing the unique capabilities of the SMEA to combine long-term electrophysiological recording with mechanical stimulation, we investigated the effect of mild-to-moderate mechanical stretch injury on bicuculline-induced, long-lasting network synchronization.

Our SMEA system has the potential to engender novel experimental strategies to investigate the mechanisms of mechanotransduction underlying the functional consequences of TBI. Compared to more labor-intensive *in vivo* approaches, the ability to test TBI hypotheses within a single organotypic slice culture over extended durations could increase the speed of drug discovery through high-content screening.[36]

## Methods

### Stretchable microelectrode arrays

Design, fabrication, and packaging of SMEAs have been described previously in detail.[37–39] Briefly, thin-film conductors (3 nm of chromium, followed by 75 nm of gold, finished with 3 nm of chromium) were sequentially deposited on a 280-$\mu$m-thick layer of polydimethylsiloxane (PDMS; Sylgard 184; Dow Corning, Midland, MI) by electron beam evaporation.[40] The gold thin-film was patterned into recording electrodes and encapsulated with a 15-$\mu$m-thick layer of either PDMS or photo-patternable silicone (WL5150; Dow Corning). Vias were opened in the encapsulation layer to expose the recording electrodes and peripheral contacts. Platinum black was electroplated on the surfaces of the recording electrodes. The SMEA was sandwiched between two printed circuit boards with circular openings for the culture well and to allow incorporation into our *in vitro* TBI model.[41] The SMEA featured 28 recording electrodes (feature size, <100 $\mu$m), two reference electrodes, and 30 peripheral contacts (Fig. 1).[38]

### Organotypic slice cultures of the rat hippocampus

All animal procedures were approved by the Columbia University Institutional Animal Care and Use Committee (New York, NY). Before plating organotypic hippocampal slice cultures, SMEAs were made hydrophilic with air-gas plasma treatment (Harrick PDC-32G; Harrick Scientific, Pleasantville, NY) for 90 sec.[42] SMEAs were precoated overnight with 80 $\mu$g/mL of laminin (Life Technologies, Carlsbad, CA) and 320 $\mu$g/mL of poly-L-lysine (Sigma-Aldrich, St. Louis, MO) and then incubated overnight with Neurobasal medium (supplemented with 1 mM of Glutamax, 50×B27, 4.5 mg/mL of D-glucose, and 10 mM of HEPES; Life Technologies) in a standard cell-culture incubator (37°C, 5% $CO_2$). Brains of postnatal day 8–11 Sprague-Dawley rat pups were aseptically removed and the hippocampus cut into 375-$\mu$m-thick slices using a McIlwain tissue chopper (Harvard Apparatus, Holliston, MA), according to published methods.[41] Hippocampal slice cultures were then plated onto precoated SMEAs and fed every 2–3 days with conditioned full-serum medium (Sigma-Aldrich; 50% minimum essential media, 25% Hank's balanced salt solution, 25% heat inactivated horse serum, 1 mM of Glutamax, 4.5 mg/mL of D-glucose, and 10 mM of HEPES) for 8–18 days total. To verify slice culture health before injury, the fluorescent dye, propidium iodide (Life Technologies), was used to stain for dead or injured cells. Unhealthy slice cultures were not included in the study, according to published methods.[43]
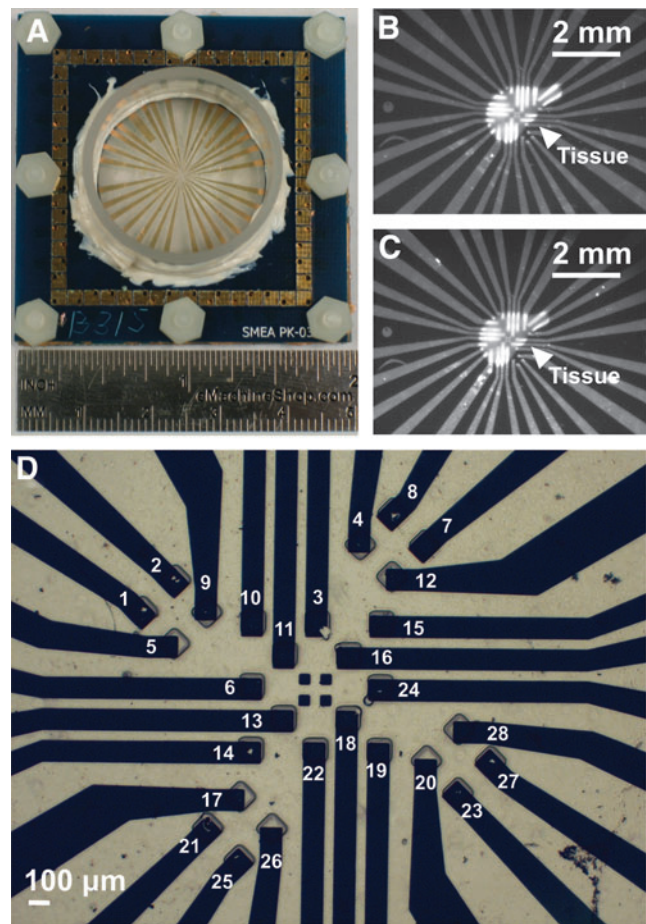


**FIG. 1.** Images of an SMEA. (**A**) The SMEA featured 28 electrodes and two reference electrodes in a 49×49 mm package. (**B**) Image of a hippocampal slice culture on an SMEA before stretch injury. (**C**) Image of a hippocampal slice culture on an SMEA after stretch injury of approximately 0.2 strain and 2 s$^{-1}$ strain rate. (**D**) Image of the 28-electrode array in the center of the SMEA. The tips of the patterned conductors were exposed through 100×100 $\mu$m vias photopatterned in the encapsulation layer. The four small squares in the center are registration marks for aligning photolithographic masks. Individual electrode ID assignments are indicated in white. SMEA, stretchable microelectrode array. Color image is available online at www.liebertpub.com/neu

### Mechanical stretch injury of hippocampal slice cultures

The *in vitro* model of mechanical stretch injury has been characterized previously in detail.[41,44] Briefly, after 8–18 days *in vitro*, media were removed from the SMEA well and the hippocampal slice cultures were mechanically stretched by pulling the SMEA over a rigid, tubular indenter. Slice culture electrophysiological function was then assessed as described below. Induced tissue strain and strain rate were verified with high-speed video analysis of the dynamic stretch injury event. Lagrangian strain was determined by calculating the deformation gradient tensor by locating fiducial markers on the tissue slice image before and at maximal stretch.[44]

### Assessment of electrophysiological function

At the indicated time point after stretch injury and while still adhered to the SMEA, slice cultures were perfused with artificial cerebrospinal fluid (aCSF; 125 mM of NaCl, 3.5 mM of KCl,

26 mM of $NaHCO_3$, 1.2 mM of $KH_2PO_4$, 1.3 mM of $MgCl_2$, 2.4 mM of $CaCl_2$, 10 mM of D-glucose, pH = 7.4; Sigma-Aldrich) at 37°C and aerated with 95% $O_2$/5% $CO_2$, as previously described.[17] For experiments involving GABA inhibition, slice cultures were perfused for a minimum of 3 min with bicuculline methiodide (50 $\mu$M; Sigma-Aldrich) in aCSF before recording electrical activity, within 1 h postinjury. Bicuculline was then washed from slice cultures for at least 20 min before returning them to the incubator for follow-up recordings at the indicated time points.

Spontaneous neural activity was measured by recording continuously for 3 min at a sampling rate of 20 kHz from all electrodes within the hippocampus before injury and at the indicated time point. Raw data were low-pass filtered with a 6-kHz analog, anti-aliasing filter and passed through a 60-Hz comb filter using a custom MATLAB script (version R2012a; MathWorks, Natick, MA). Consistent with other MEA studies with acute slices, electrodes of SMEAs recorded local field potentials produced by populations of neuronal cell bodies, dendrites, and axons within the local vicinity of individual electrodes.[45] Neural event activity was detected based on the multi-resolution Teager energy operator (m-TEO), which identifies epochs of data that contain high energy in specific frequency bands that are indicative of the feature being detected.[46] In this case, the feature was the local field potential of neuronal ensembles recorded by the planar electrodes of the SMEA. The m-TEO was calculated for k = (600, 900, and 1200), and neural events were identified as the onset of those epochs with an m-TEO greater than 0.5 root mean square error (RMSE) above the baseline m-TEO and with a raw signal greater than 1.5 RMSE above the baseline of the raw signal.[47]

Using the results from the previous analysis above, which identified the onset time of each neural event on each electrode, the degree of correlation for event trains across electrode pairs was investigated. Spontaneous network synchronization was quantified using previously published methods based on correlation matrix analysis and surrogate resampling for significance testing.[48–50] Correlation of neural events was computed to determine an event synchronization measure, the synchronization index, for each electrode pair.[48] Correlated neural events across electrodes were defined as detected neural events that occurred within 1.5 ms of one another.[47] For two electrodes $x$ and $y$, and neural event timing $t_i^x$ and $t_j^y$ (i = 1,…, $m_x$; j = 1,…, $m_y$), the event correlation matrix was calculated by Equation 1:

$$c^\tau(x|y) = \sum_{i=1}^{m_x} \sum_{j=1}^{m_y} J_{ij}^\tau \begin{cases} J_{ij}^\tau = 1 & if\ 0 < t_i^x - t_j^y \leq \tau \\ J_{ij}^\tau = \frac{1}{2} & if\ t_i^x = t_j^y \\ J_{ij}^\tau = 0 & otherwise \end{cases} \quad (1)$$

where $\tau$ was the time interval in which two events were considered synchronous (1.5 ms), $m_x$ and $m_y$ were the total number of events to be compared, and $J_{ij}^\tau$ was a measure of correlation of two particular electrodes.

The event synchronization index for each electrode comparison, ranging in value from 0 (completely uncorrelated) to 1 (perfectly correlated), was calculated by Equation 2:

$$Q_\tau = \frac{c^\tau(x|y) + c^\tau(y|x)}{\sqrt{m_x m_y}} \quad (2)$$

To identify clusters of synchronized electrodes, first, the participation index (PI) was calculated for each electrode $a$ that contributed to a cluster $b$ (Equation 3):

$$PI_{ab} = \lambda_b \nu_{ab}^2 \quad (3)$$

where $v_{ab}$ was the $a^{th}$ element of eigenvector $v_b$ and $\lambda_b$ was the corresponding eigenvalue of the event correlation matrix [$c^\tau(x|y)$]. $PI_{ab}$ indicated the contribution of electrode $a$ to the synchronized

cluster $b$, with $\nu_{ab}^2$ defined as the weight with which electrode $a$ contributed to cluster $b$. Clusters were defined as groups of electrodes with statistically similar patterns of activity, defined by PI ≥ 0.01.[49]

Next, randomized surrogate time-series data without correlated electrode pairs were mathematically generated with an event rate equal to the instantaneous event rate of the experimental recordings by generating an inhomogeneous Poisson-distributed, ''event train.'' These uncorrelated, synthetic event trains were analyzed identically to the experimental data to produce a correlation matrix, eigenvalues, eigenvectors, and PI to bootstrap hypothesis testing of the experimental data.[49] Essentially, the uncorrelated Poisson-distributed event trains served as the null hypothesis against which to test experimental data. The surrogate randomization was repeated 50 times, and the mean ($\bar{\lambda}_k'$) and standard deviation ($SD_k$) of surrogate eigenvalues were calculated (k = 1,…, M, where M was the number of electrodes). We identified the number of synchronized clusters that were significantly different from the randomized, asynchronous surrogates by Equation 4:

$$Number\ of\ Clusters = \sum_k sgn[\lambda_k > (\bar{\lambda}_k' + K \times SD_k)] \quad (4)$$

where $sgn$ was a sign function, $\lambda_k$ was the eigenvalue of each electrode of the experimental data, and $K$ was a constant ($K = 3$, for 99% confidence level, was used for this study). Detection of synchronized clusters represented the presence of neuronal assemblies functioning in an organized network. It is believed that neuron assemblies play a critical role in higher-order hippocampal function, including spatial navigation and memory processes,[51] which may be disrupted post-TBI and axonal injury.[52]

The degree of synchronization can be quantified and compared across slice cultures by calculating the global synchronization index (GSI), ranging from 0 (completely random, uncorrelated activity) to 1 (perfectly synchronous, correlated activity), for the cluster with the highest degree of synchronization within each slice culture (Equation 5):

$$GSI = \begin{cases} \frac{\lambda_M - \bar{\lambda}'}{M - \bar{\lambda}'} & if\ \lambda_M > \bar{\lambda}' \\ 0 & otherwise \end{cases} \quad (5)$$

where $\bar{\lambda}'$ was the mean of the highest eigenvalues calculated across all surrogates, $\lambda_M$ was the maximal eigenvalue of the correlation matrix from the experimental data, and $M$ was the number of electrodes. Lower synchronization (i.e., lower GSI) has been associated with dysfunctional or damaged neural networks.[53] Last, the GSI was apportioned to each region (dentate gyrus [DG], cornu amonis [CA]3, and CA1) based on the fraction of regional electrodes participating in the cluster to obtain a normalized GSI for each region.

### Statistical analysis

To account for variability in the density and excitability of neuronal populations at each electrode, spontaneous activity data were normalized to preinjury levels for neural event rate on an electrode-by-electrode basis. Spontaneous activity and network synchronization data were analyzed by analysis of variance, followed by Bonferroni's post-hoc tests with statistical significance set as $p < 0.05$.

## Results

### Mechanical injury alone did not alter spontaneous network activity

For all injured slice cultures, the average Lagrangian strain was $0.22 \pm 0.02$ and the average strain rate was $2.37 \pm 0.39\ s^{-1}$ ($n = 12$ slice cultures, mean ± SD), which constituted a mild-to-moderate injury as
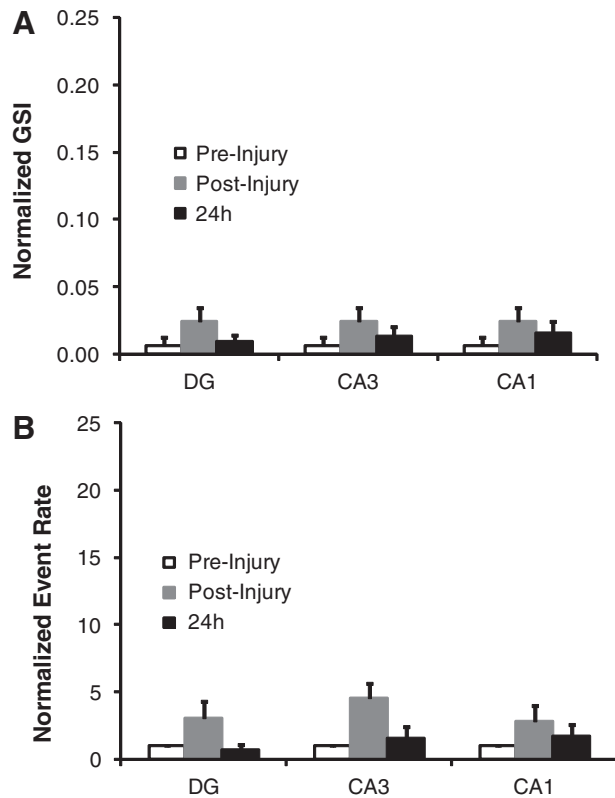
FIG. 2. Neither network synchronization of spontaneous activity nor the normalized spontaneous event rate was significantly affected by injury. (**A**) Network synchronization, as measured by the normalized global synchronization index (GSI), was not significantly affected by injury either acutely or 24 h postinjury in DG, CA3, or CA1. (**B**) The normalized spontaneous event rate was not significantly altered by injury in DG, CA3, or CA1, either acutely postinjury or 24 h postinjury. All data were normalized to preinjury, pretreatment levels (mean ± standard error of the mean). DG, dentate gyrus; CA, cornu amonis.

previously reported.[17–19] Cell death was consistent with previously reported cell death in hippocampal slice cultures caused by mild-to-moderate injury.[19] Immediately postinjury and 24 h postinjury, no significant change in normalized GSI was observed in any region (Fig. 2A). In addition, no significant alterations in normalized spontaneous event rate were observed in any region either acutely or 24 h postinjury (Fig. 2B). These results are consistent with the mild-to-moderate severity of the injury and the recording time point.[17,31]

*Mechanical injury disrupted bicuculline-induced,*
*long-lasting network synchronization*

In both uninjured and injured slice cultures, bicuculline induced highly synchronized, correlated neural activity (Fig. 3A,B). Before injury or bicuculline treatment, the hippocampal network was not synchronized, as denoted by low (blue) correlation coefficients (Fig. 4A,D). During bicuculline treatment, network synchronization increased in both uninjured and injured slice cultures (Fig. 4B,E). Twenty-four hours after bicuculline treatment, the hippocampal network remained highly synchronized in uninjured slice cultures (Fig. 4C), whereas in injured cultures synchrony was significantly decreased (Fig. 4F).

Before injury or bicuculline treatment, the normalized GSI was very low in all regions of both uninjured and injured slice cultures
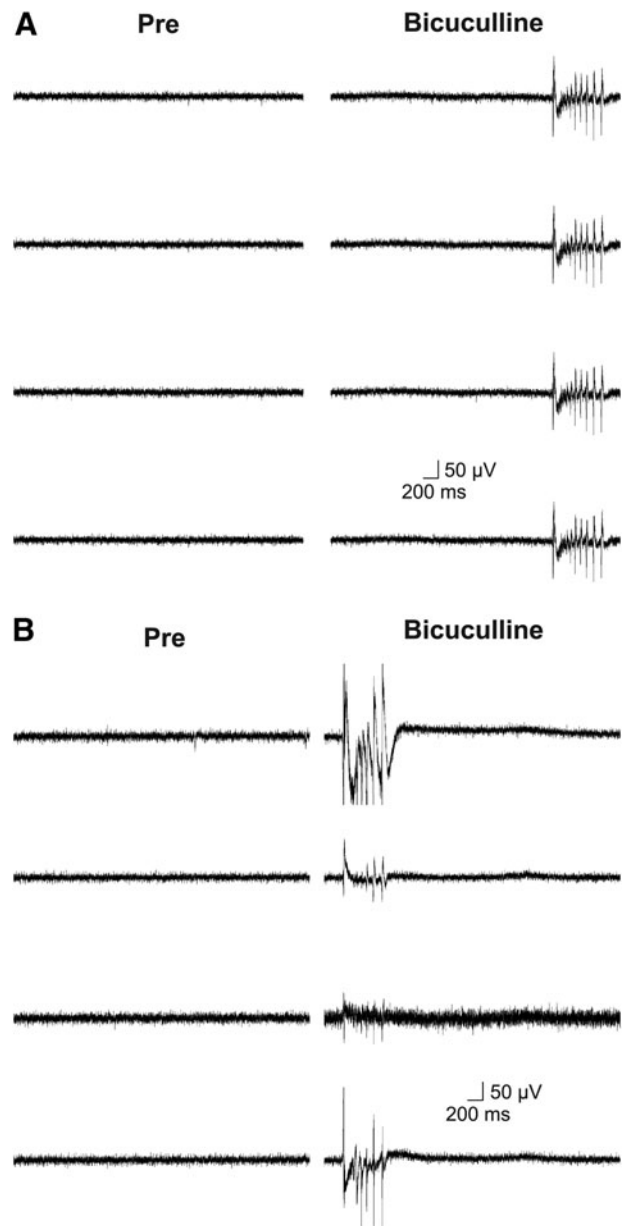


FIG. 3. Representative traces of temporally aligned raw electrophysiology data from four electrodes in CA1 before bicuculline treatment and during bicuculline treatment from uninjured (**A**) and injured (**B**) slice cultures.

(Fig. 5; normalized GSI, < 0.01). During bicuculline treatment, normalized GSI significantly increased in all regions in both uninjured and injured cultures. Twenty-four hours after bicuculline treatment, normalized GSI was significantly higher in uninjured cultures, compared to prebicuculline levels and compared to injured cultures. In contrast, in all regions of injured cultures, normalized GSI was significantly decreased, compared to during bicuculline treatment.

*Mechanical injury increased the rate*
*of bicuculline-induced spontaneous activity*

In all regions of uninjured slice cultures, no significant alteration in the normalized spontaneous event rate was observed 24 h after
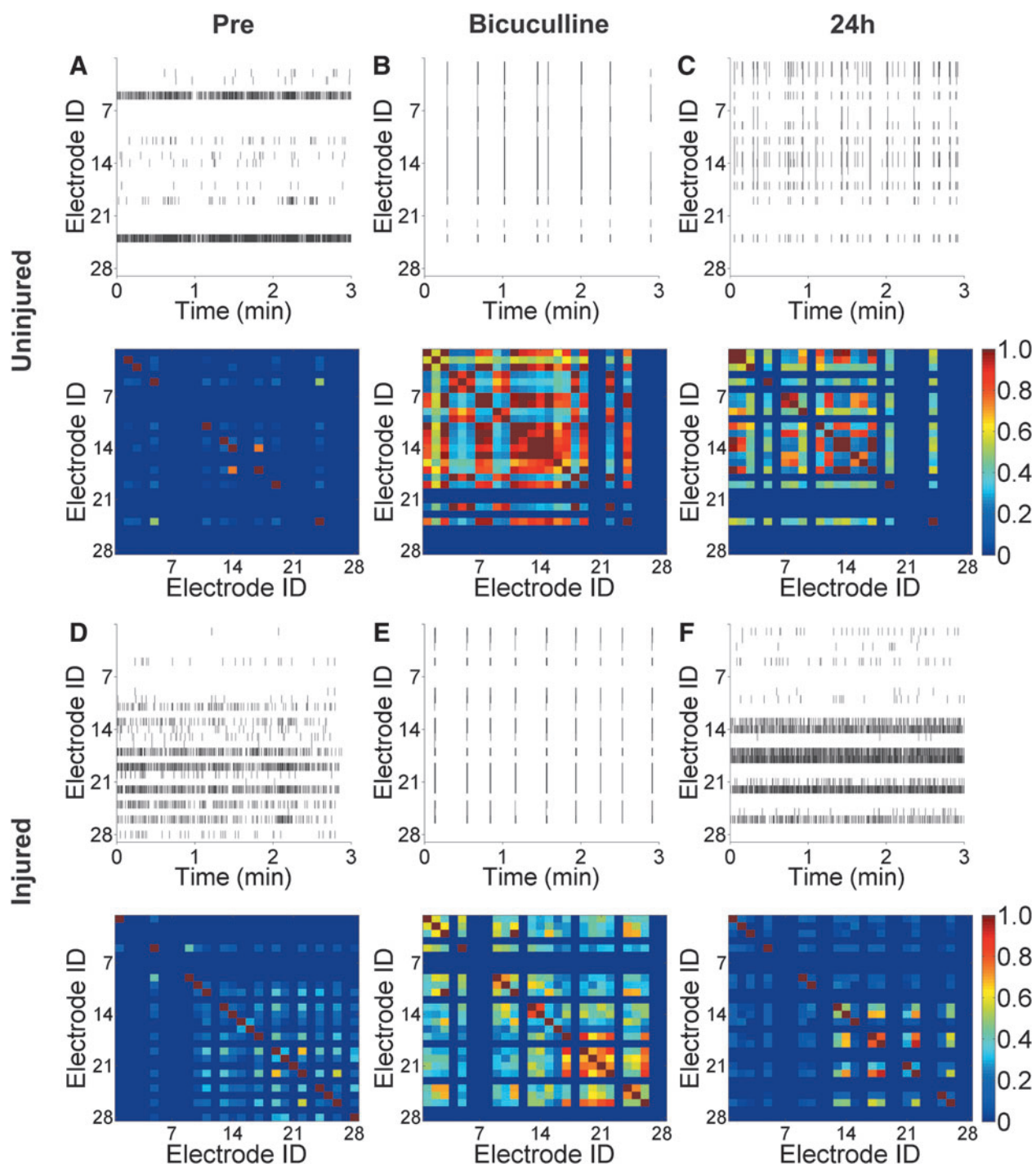
**FIG. 4.** Changes in bicuculline-induced, long-lasting network synchronization of spontaneous activity in uninjured and injured slice cultures. Representative raster plots of spontaneous activity and heat maps of pair-wise synchronization $c^\tau(x|y)$ for every electrode pair are shown for uninjured and injured slice cultures at the indicated time points: preinjury (or sham exposure) and before bicuculline treatment (**A** and **D**), during bicuculline treatment (**B** and **E**), and 24 h after bicuculline treatment (**C** and **F**). Each line in the raster plots represent a distinct, identified neural event. Heat maps of pair-wise synchronization depict the event synchronization index for each electrode pair, ranging in value from 0 (completely uncorrelated, blue) to 1 (perfectly correlated, red). Color image is available online at www.liebertpub.com/neu

bicuculline exposure (Fig. 6A–C). However, 24 h after bicuculline exposure of injured slice cultures, normalized spontaneous event rate was significantly increased in DG and CA1, compared to preinjury, pretreatment levels, as well as when compared to uninjured cultures at the same time point (Fig.

6A,C). No significant changes were observed in CA3 (Fig. 6B). These results suggest that mild-to-moderate injury affected the ability of the surviving neuronal network to synchronize activity and not simply the ability of neurons to generate activity.

*Effects of bicuculline re-exposure differed by hippocampal region*

Twenty-four hours after the initial bicuculline treatment, injured slice cultures were exposed to bicuculline a second time to probe for potential mechanisms of the disruption in bicuculline-induced, long-lasting network synchronization. Re-exposure to bicuculline significantly increased normalized GSI in all hippocampal regions,

compared to preinjury, pretreatment baseline levels and compared to 24 h after the initial postinjury bicuculline exposure (Fig. 7A). In contrast, the effect of re-exposure to bicuculline on event rate was region dependent, significantly decreasing spontaneous activity in the DG, but significantly increasing it in CA3 and CA1 (Fig. 7B).

## Discussion

In the present study, bicuculline exposure almost immediately transformed the network activity of both uninjured and injured hippocampal slice cultures from random, asynchronous activity to highly synchronized, correlated neural activity (Fig. 3). In uninjured cultures, this coordinated activity persisted for at least 24 h after removal of bicuculline (Fig. 4). In contrast, this long-lasting network synchronization was not evident in cultures that were mechanically injured (Fig. 5A–C), despite increased network synchronization during bicuculline exposure and despite increased asynchronous activity 24 h after bicuculline exposure (Fig. 6A–C).

Injury severity for this study was chosen to be characteristic of mild-to-moderate TBI, which causes neuronal network dysfunction without appreciable cell death.[17] We observed that mechanical injury disrupted bicuculline-induced, long-lasting network synchronization, but did not abolish neuronal network activity (Figs. 4–6). In fact, the normalized spontaneous event rate was higher in the DG and CA1 24 h after injury (Fig. 6A,C). Despite the hippocampal neuronal network being even more active after injury, it was unable to maintain synchronized, correlated activity, a deficit that could explain learning and memory impairments post-TBI because the neural process underlying information storage in working memory is persistent neural activity.[12] During memory encoding and recognition, optimally functional neuronal networks are highly organized and exhibit synchronization between interconnected neuronal regions.[54] Brain dysfunction postinjury, such as mild TBI (mTBI),[53] or as a result of neurological disorders, such as Alzheimer's disease,[55] alters the functional structure of neuronal networks, transforming synchronized networks into less-ordered, more-random networks. In patients tested within days of suffering an mTBI, global synchronization and network organization of rhythmic brain activity hypothesized to underlie episodic memory, was reduced, as measured by electroencephalography recordings.[53] These patients also exhibited reduced performance in visual recognition tasks that were dependent on short-term episodic memory.
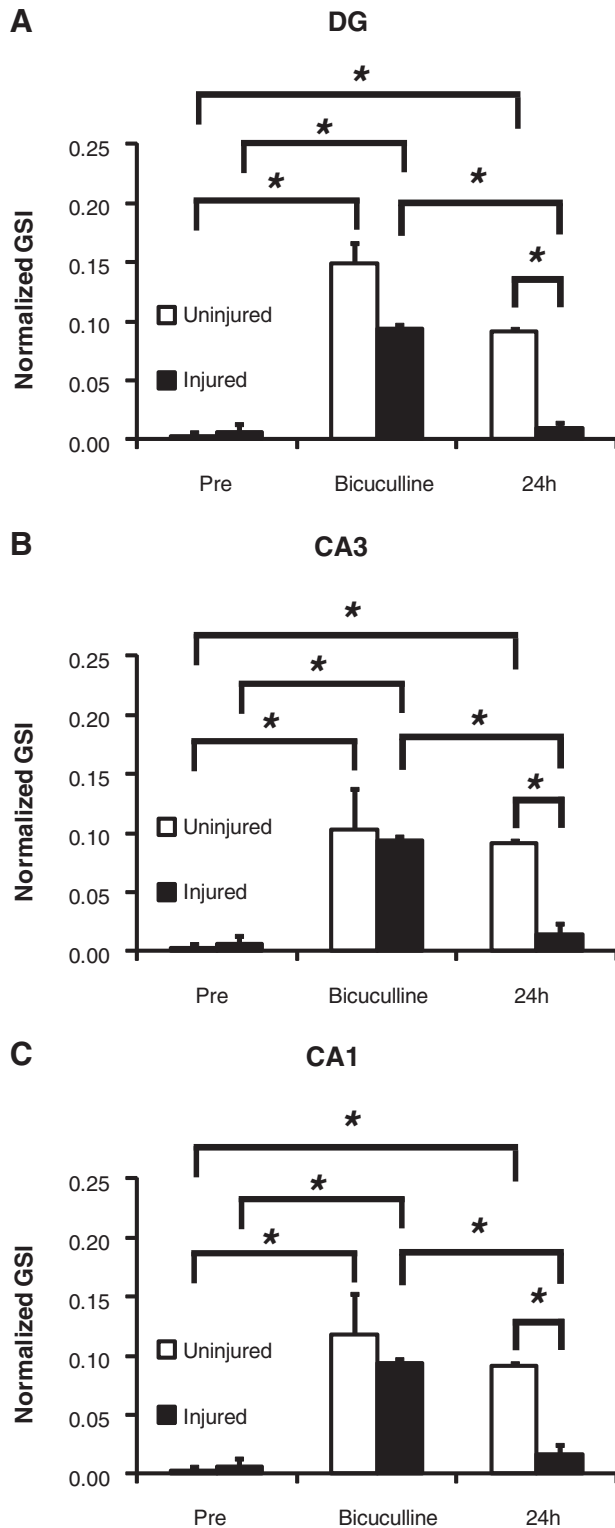


**FIG. 5.** Changes in bicuculline-induced, long-lasting network synchronization of spontaneous activity in uninjured and injured slice cultures, quantified by the normalized GSI. Preinjury (or sham exposure) and bicuculline treatment, network activity was not synchronized in any region (DG, CA3, or CA1), with the normalized GSI below 0.01 (**A–C**). Acutely during bicuculline exposure, the normalized GSI increased significantly in all hippocampal regions in both uninjured and injured slice cultures, compared to their respective baseline recordings, indicating significantly higher network synchronization. Twenty-four hours after bicuculline exposure, the normalized GSI remained significantly higher in all hippocampal regions in uninjured slice cultures, compared to pretreatment baseline levels. In all regions of injured slice cultures, the normalized GSI was significantly diminished 24 h after bicuculline exposure, when compared to the normalized GSI during bicuculline treatment, and when compared to uninjured slice cultures 24 h after bicuculline treatment. Data are presented as mean ± standard error of the mean. GSI, global synchronization index; DG, dentate gyrus; CA, cornu amonis.
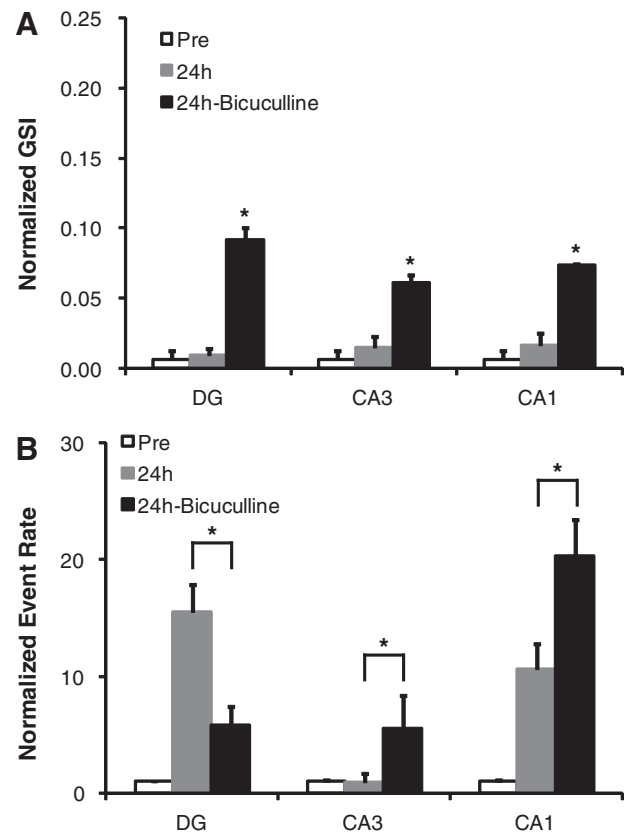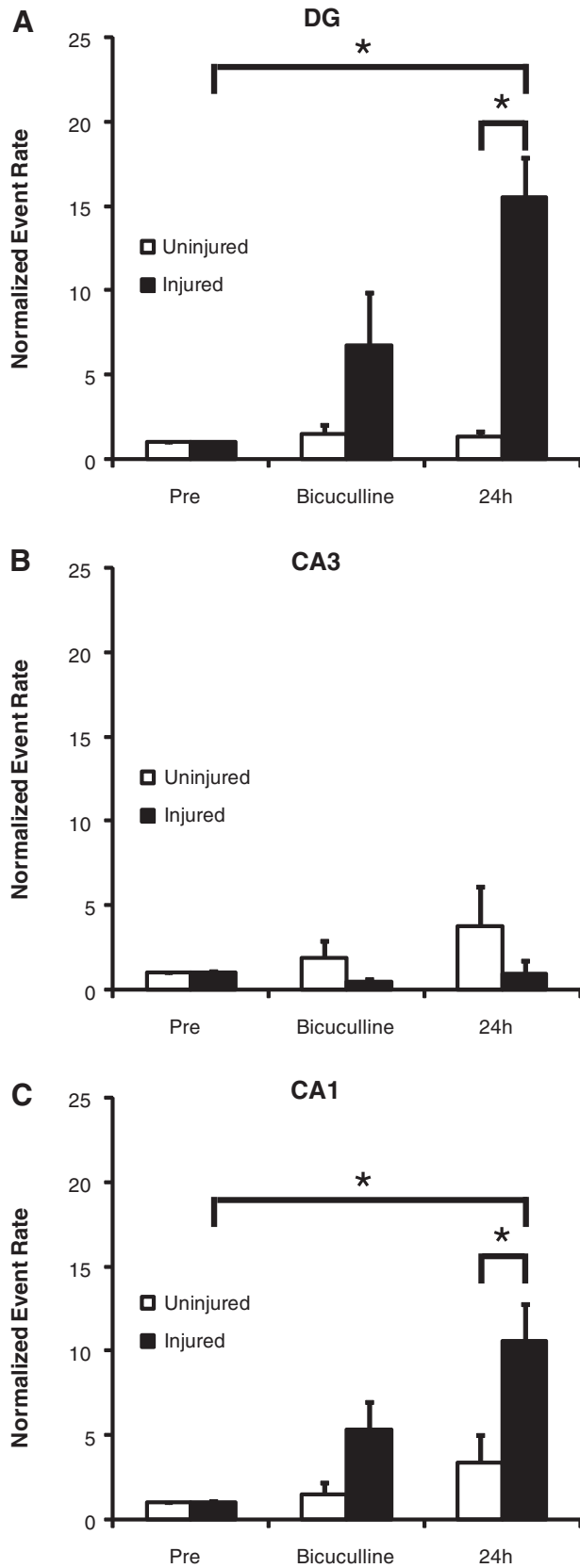
**FIG. 7.** Changes in network synchronization of spontaneous activity and the normalized spontaneous event rate in injured slice cultures. (**A**) Second exposure to bicuculline 24 h after the initial bicuculline exposure significantly increased the normalized GSI compared to preinjury, pretreatment baseline levels and compared to 24 h postinjury and the initial bicuculline exposure in DG, CA3, and CA1. The normalized GSI was not significantly different between hippocampal regions after the second bicuculline exposure. (**B**) Second exposure to bicuculline 24 h after the initial bicuculline exposure produced different effects on the normalized spontaneous event rate depending on hippocampal region. Compared to 24 h, re-exposure to bicuculline significantly decreased the normalized spontaneous event rate in DG, while significantly increasing the normalized spontaneous event rate in CA3 and CA1. All data were normalized to preinjury, pretreatment levels (mean ± standard error of the mean). GSI, global synchronization index; DG, dentate gyrus; CA, cornu amonis.

It is an interesting observation that, in the current study, stretch disrupted the development of long-lasting network synchronization *in vitro* as well.[53]

Exposing injured slice cultures to a second bicuculline challenge 24 h after the initial exposure resulted in region-dependent changes



**FIG. 6.** Normalized spontaneous event rate before and after bicuculline treatment in uninjured and injured slice cultures. Twenty-hour hours after bicuculline exposure, the normalized spontaneous event rate was significantly increased in injured DG (**A**) and CA1 (**C**) compared to pretreatment, preinjury baseline levels and compared to uninjured DG and CA1 at the same time point. No significant changes in the normalized spontaneous event rate were observed in CA3 (**B**). All data were normalized to preinjury, pretreatment levels (mean ± standard error of the mean). DG, dentate gyrus; CA, cornu amonis.

in normalized event rate (Fig. 7). We speculate that the underlying mechanism behind this region-dependent observation may involve the interplay between the K-Cl cotransporter (KCC2) and the Na-K-2Cl cotransporter (NKCC1) in regulating the concentration of intracellular chloride. KCC2 has been implicated to play a key role in the impairment of GABAergic inhibition after mechanical injury.[56] Bonislawski and colleagues observed significantly reduced KCC2 expression post-TBI and a concomitant depolarized shift of the normally hyperpolarizing GABA$_A$ reversal potential in DG, but not CA1. Additionally, in a separate study, significant enhancement of spontaneous circuit activity in cultured hippocampal neurons was observed after pharmacological inhibition of KCC2.[57] With the depolarizing shift in the GABA$_A$ reversal potential owing to post-injury alterations in KCC2 expression, GABA neurotransmission may become depolarizing/excitatory, rather than hyperpolarizing/inhibitory, thereby increasing spontaneous activity postinjury. In this case, inhibition of GABA by bicuculline would then be hypothesized to decrease spontaneous activity, which may help explain our observations in the DG after injury (Fig. 7). In general, however, chloride gradients shift by changing the expression of NKCC1 and KCC2 in the second week of development in rodents.[58] The hippocampal slice cultures used in our experiments were generated from postnatal day 8–11 rat pups and were further cultured for an additional 18 days. Future experiments will be necessary to directly test whether changes in expression or activity of KCC2 and NKCC1 are responsible for these post-traumatic changes in network function. Quantifying the changes in NKCC1 and KCC2 protein expression before and after injury may uncover region-dependent roles of the chloride transporters within the hippocampus.

Significant progress has been made in improving the fabrication process of the SMEA and reducing the size of the recording contacts from $300 \times 300\,\mu m$ to $100 \times 100\,\mu m$, nearly 90% smaller compared to earlier generations.[38] The reduced feature size has allowed for an increase in the number of recording electrodes from 11 to 28 (12–30 electrodes total, including reference electrodes) over the same surface area. However, a continuing limitation of the SMEA is the relatively large feature size of the recording electrodes, compared to individual neurons. Commercially available rigid MEAs feature electrodes as small as $8\,\mu m$ in diameter (256MEA30/8iR-ITO; Multi Channel Systems MCS GmbH, Reutlingen, Germany). Currently, multiple neurons and neuronal ensembles may contribute to the summed signal measured from a single electrode. Smaller electrodes could potentially allow for stimulation and recording of individual neurons, increasing the spatial resolution of SMEA-based studies. Although the fabrication process remains difficult and expensive, efforts are underway to improve it and reduce overall manufacturing costs. In addition, *in vitro* slice cultures do not precisely recapitulate important factors of the *in vivo* extracellular environment, such as oxygenation and interplay with systemic blood supply.[25] Components of these systemic factors can be added to an *in vitro* slice culture model, but would require further characterization in order to limit any confounding effects.

### Acknowledgments

### Author Disclosure Statement

Oliver Graudejus is president of BMSEED, LLC, which is trying to commercialize the SMEA technology. No other competing financial interests exist.

### References

1. Gean, A.D., and Fischbein, N.J. (2010). Head trauma. Neuroimaging Clin. N. Am. 20, 527–556.
2. Hyder, A.A., Wunderlich, C.A., Puvanachandra, P., Gururaj, G., and Kobusingye, O.C. (2007). The impact of traumatic brain injuries: a global perspective. NeuroRehabilitation 22, 341–353.
3. Faul, M., Xu, L., Wald, M.M., Coronado, V., and Dellinger, A.M. (2010). Traumatic Brain Injury in the United States: National Estimates of Prevalence and Incidence, 2002–2006. Injury Prev. 16, A268–A268.
4. Kinnunen, K.M., Greenwood, R., Powell, J.H., Leech, R., Hawkins, P.C., Bonnelle, V., Patel, M.C., Counsell, S.J., and Sharp, D.J. (2011). White matter damage and cognitive impairment after traumatic brain injury. Brain 134, 449–463.
5. Christidi, F., Bigler, E.D., McCauley, S.R., Schnelle, K.P., Merkley, T.L., Mors, M.B., Li, X., Macleod, M., Chu, Z., Hunter, J.V., Levin, H.S., Clifton, G.L., and Wilde, E.A. (2011). Diffusion tensor imaging of the perforant pathway zone and its relation to memory function in patients with severe traumatic brain injury. J. Neurotrauma 28, 711–725.
6. Ommaya, A.K., and Gennarelli, T.A. (1974). Cerebral concussion and traumatic unconsciousness. Correlation of experimental and clinical observations of blunt head injuries. Brain 97, 633–654.
7. Fujimoto, S.T., Longhi, L., Saatman, K.E., Conte, V., Stocchetti, N., and McIntosh, T.K. (2004). Motor and cognitive function evaluation following experimental traumatic brain injury. Neurosci. Biobehav. Rev. 28, 365–378.
8. Margulies, S.S., and Thibault, L.E. (1989). An analytical model of traumatic diffuse brain injury. J. Biomech. Eng. 111, 241–249.
9. Asikainen, I., Kaste, M., and Sarna, S. (1999). Early and late post-traumatic seizures in traumatic brain injury rehabilitation patients: brain injury factors causing late seizures and influence of seizures on long-term outcome. Epilepsia 40, 584–589.
10. Sosin, D.M., Sniezek, J.E., and Waxweiler, R.J. (1995). Trends in death associated with traumatic brain injury, 1979 through 1992. Success and failure. JAMA 273, 1778–1780.
11. Hoskison, M.M., Moore, A.N., Hu, B., Orsi, S., Kobori, N., and Dash, P.K. (2009). Persistent working memory dysfunction following traumatic brain injury: evidence for a time-dependent mechanism. Neuroscience 159, 483–491.
12. Wang, X.J. (2001). Synaptic reverberation underlying mnemonic persistent activity. Trends Neurosci. 24, 455–463.
13. Buzsaki, G. (1989). Two-stage model of memory trace formation: a role for ''noisy'' brain states. Neuroscience 31, 551–570.
14. Kobori, N., and Dash, P.K. (2006). Reversal of brain injury-induced prefrontal glutamic acid decarboxylase expression and working memory deficits by D1 receptor antagonism. J. Neurosci. 26, 4236–4246.
15. Levin, H.S., Hanten, G., Chang, C.C., Zhang, L., Schachar, R., Ewing-Cobbs, L., and Max, J.E. (2002). Working memory after traumatic brain injury in children. Ann. Neurol. 52, 82–88.
16. McAllister, T.W., Saykin, A.J., Flashman, L.A., Sparling, M.B., Johnson, S.C., Guerin, S.J., Mamourian, A.C., Weaver, J.B., and Yanofsky, N. (1999). Brain activation during working memory 1 month after mild traumatic brain injury: a functional MRI study. Neurology 53, 1300–1308.
17. Yu, Z., and Morrison, B. 3rd. (2010). Experimental mild traumatic brain injury induces functional alteration of the developing hippocampus. J. Neurophysiol. 103, 499–510.
18. Elkin, B.S., and Morrison, B. 3rd. (2007). Region-specific tolerance criteria for the living brain. Stapp Car Crash J. 51, 127–138.
19. Cater, H.L., Sundstrom, L.E., and Morrison, B. 3rd. (2006). Temporal development of hippocampal cell death is dependent on tissue strain but not strain rate. J. Biomech. 39, 2810–2818.

20. Viano, D.C., Casson, I.R., Pellman, E.J., Zhang, L., King, A.I., and Yang, K.H. (2005). Concussion in professional football: brain responses by finite element analysis: part 9. Neurosurgery 57, 891–916; discussion, 891–916.

21. Kleiven, S. (2007). Predictors for traumatic brain injuries evaluated through accident reconstructions. Stapp Car Crash J. 51, 81–114.

22. Hardy, W.N., Mason, M.J., Foster, C.D., Shah, C.S., Kopacz, J.M., Yang, K.H., King, A.I., Bishop, J., Bey, M., Anderst, W., and Tashman, S. (2007). A study of the response of the human cadaver head to impact. Stapp Car Crash J. 51, 17–80.

23. Bayly, P.V., Cohen, T.S., Leister, E.P., Ajo, D., Leuthardt, E.C., and Genin, G.M. (2005). Deformation of the human brain induced by mild acceleration. J. Neurotrauma 22, 845–856.

24. Bayly, P.V., Black, E.E., Pedersen, R.C., Leister, E.P., and Genin, G.M. (2006). In vivo imaging of rapid deformation and strain in an animal model of traumatic brain injury. J. Biomech. 39, 1086–1095.

25. Morrison, B. 3rd, Elkin, B.S., Dolle, J.P., and Yarmush, M.L. (2011). In vitro models of traumatic brain injury. Annu. Rev. Biomed. Eng. 13, 91–126.

26. Morrison, B. 3rd, Saatman, K.E., Meaney, D.F., and McIntosh, T.K. (1998). In vitro central nervous system models of mechanically induced trauma: a review. J. Neurotrauma 15, 911–928.

27. Beggs, J.M., and Plenz, D. (2004). Neuronal avalanches are diverse and precise activity patterns that are stable for many hours in cortical slice cultures. J. Neurosci. 24, 5216–5229.

28. Arnold, F.J., Hofmann, F., Bengtson, C.P., Wittmann, M., Vanhoutte, P., and Bading, H. (2005). Microelectrode array recordings of cultured hippocampal networks reveal a simple model for transcription and protein synthesis-dependent plasticity. J. Physiol. 564, 3–19.

29. Kralik, J.D., Dimitrov, D.F., Krupa, D.J., Katz, D.B., Cohen, D., and Nicolelis, M.A. (2001). Techniques for long-term multisite neuronal ensemble recordings in behaving animals. Methods 25, 121–150.

30. Doetsch, G.S. (2000). Patterns in the brain. Neuronal population coding in the somatosensory system. Physiol. Behav. 69, 187–201.

31. Yu, Z., Graudejus, O., Tsay, C., Lacour, S.P., Wagner, S., and Morrison, B. 3rd. (2009). Monitoring hippocampus electrical activity in vitro on an elastically deformable microelectrode array. J. Neurotrauma 26, 1135–1145.

32. Matsuyama, S., Taniguchi, T., Kadoyama, K., and Matsumoto, A. (2008). Long-term potentiation-like facilitation through GABAA receptor blockade in the mouse dentate gyrus in vivo. Neuroreport 19, 1809–1813.

33. Sloviter, R.S. (1994). On the relationship between neuropathology and pathophysiology in the epileptic hippocampus of humans and experimental animals. Hippocampus 4, 250–253.

34. De Curtis, M., Biella, G., Forti, M., and Panzica, F. (1994). Multifocal spontaneous epileptic activity induced by restricted bicuculline ejection in the piriform cortex of the isolated guinea pig brain. J. Neurophysiol. 71, 2463–2476.

35. Li, X., Zhou, W., Zeng, S., Liu, M., and Luo, Q. (2007). Long-term recording on multi-electrode array reveals degraded inhibitory connection in neuronal network development. Biosens. Bioelectron. 22, 1538–1543.

36. Sundstrom, L., Morrison, B. 3rd, Bradley, M. and Pringle, A. (2005). Organotypic cultures as tools for functional screening in the CNS. Drug Discov. Today 10, 993–1000.

37. Lacour, S.P., Wagner, S., Huang, Z.Y., and Suo, Z. (2003). Stretchable gold conductors on elastomeric substrates. Appl. Phys. Lett. 82, 2404–2406.

38. Graudejus, O., Morrison, B., Goletiani, C., Yu, Z., and Wagner, S. (2012). Encapsulating elastically stretchable neural interfaces: yield, resolution, and recording/stimulation of neural activity. Adv. Funct. Mater. 22, 640–651.

39. Tsay, C., Lacour, S.P., Wagner, S., and Morrison, B. (2005). Architecture, fabrication, and properties of stretchable micro-electrode arrays. Proc. 4th IEEE Conf. Sensors, 1169–1172.

40. Graudejus, O., Yu, Z., Jones, J., Morrison, B., and Wagner, S. (2009). Characterization of an elastically stretchable microelectrode array and its application to neural field potential recordings. J. Electrochem. Soc. 156, P85–P94.

41. Morrison, B. 3rd, Cater, H.L., Benham, C.D., and Sundstrom, L.E. (2006). An in vitro model of traumatic brain injury utilising two-dimensional stretch of organotypic hippocampal slice cultures. J. Neurosci. Methods 150, 192–201.

42. Egert, U., and Meyer, T. (2005). Heart on a chip—extracellular multielectrode recordings from cardiac myocytes in vitro, in: *Practical Methods in Cardiovascular Research*. S. Dhein, F. Mohr, and M. Delmar (eds). Springer: Berlin; Heidelberg, pps. 432–453.

43. Effgen, G.B., Hue, C.D., Vogel, E. 3rd, Panzer, M.B., Meaney, D.F., Bass, C.R. and Morrison, B. 3rd. (2012). A multiscale approach to blast neurotrauma modeling: part II: methodology for inducing blast injury to in vitro models. Front. Neurol. 3, 23.

44. Morrison, B. 3rd, Cater, H.L., Wang, C.C., Thomas, F.C., Hung, C.T., Ateshian, G.A., and Sundstrom, L.E. (2003). A tissue level tolerance criterion for living brain developed with an in vitro model of traumatic mechanical loading. Stapp Car Crash J. 47, 93–105.

45. Novak, J.L., and Wheeler, B.C. (1988). Multisite hippocampal slice recording and stimulation using a 32 element microelectrode array. J. Neurosci. Methods 23, 149–159.

46. Choi, J.H., Jung, H.K., and Kim, T. (2006). A new action potential detector using the MTEO and its effects on spike sorting systems at low signal-to-noise ratios. IEEE Trans. Biomed. Eng. 53, 738–746.

47. Pimashkin, A., Kastalskiy, I., Simonov, A., Koryagina, E., Mukhina, I., and Kazantsev, V. (2011). Spiking signatures of spontaneous activity bursts in hippocampal cultures. Front. Comput Neurosci. 5, 46.

48. Li, X., Cui, D., Jiruska, P., Fox, J.E., Yao, X., and Jefferys, J.G. (2007). Synchronization measurement of multiple neuronal populations. J. Neurophysiol. 98, 3341–3348.

49. Li, X., Ouyang, G., Usami, A., Ikegaya, Y., and Sik, A. (2010). Scale-free topology of the CA3 hippocampal network: a novel method to analyze functional neuronal assemblies. Biophys. J. 98, 1733–1741.

50. Patel, T.P., Ventre, S.C., and Meaney, D.F. (2012). Dynamic changes in neural circuit topology following mild mechanical injury in vitro. Ann. Biomed. Eng. 40, 23–36.

51. Bahner, F., Weiss, E.K., Birke, G., Maier, N., Schmitz, D., Rudolph, U., Frotscher, M., Traub, R.D., Both, M., and Draguhn, A. (2011). Cellular correlate of assembly formation in oscillating hippocampal networks in vitro. Proc. Natl. Acad. Sci. U. S. A. 108, E607–E616.

52. Sharp, D.J., Scott, G., and Leech, R. (2014). Network dysfunction after traumatic brain injury. Nat. Rev. Neurol. 10, 156–166.

53. Tsirka, V., Simos, P.G., Vakis, A., Kanatsouli, K., Vourkas, M., Erimaki, S., Pachou, E., Stam, C.J., and Micheloyannis, S. (2011). Mild traumatic brain injury: graph-model characterization of brain networks for episodic memory. Int. J. Psychophysiol. 79, 89–96.

54. Stam, C.J., Jones, B.F., Nolte, G., Breakspear, M., and Scheltens, P. (2007). Small-world networks and functional connectivity in Alzheimer's disease. Cereb. Cortex 17, 92–99.

55. Stam, C.J., de Haan, W., Daffertshofer, A., Jones, B.F., Manshanden, I., van Cappellen van Walsum, A.M., Montez, T., Verbunt, J.P., de Munck, J.C., van Dijk, B.W., Berendse, H.W., and Scheltens, P. (2009). Graph theoretical analysis of magnetoencephalographic functional connectivity in Alzheimer's disease. Brain 132, 213–224.

56. Bonislawski, D.P., Schwarzbach, E.P., and Cohen, A.S. (2007). Brain injury impairs dentate gyrus inhibitory efficacy. Neurobiol. Dis. 25, 163–169.

57. Wang, W., and Xu, T.L. (2006). Chloride homeostasis differentially affects GABA(A) receptor- and glycine receptor-mediated effects on spontaneous circuit activity in hippocampal cell culture. Neurosci. Lett. 406, 11–16.

58. Leinekugel, X., Khalilov, I., McLean, H., Caillard, O., Gaiarsa, J.L., Ben-Ari, Y., and Khazipov, R. (1999). GABA is the principal fast-acting excitatory transmitter in the neonatal brain. Adv. Neurol. 79, 189–201.

Address correspondence to:
*Barclay Morrison, III, PhD*
*Department of Biomedical Engineering*
*Columbia University*
*351 Engineering Terrace*
*MC 8904*
*1210 Amsterdam Avenue*
*New York, NY 10027*

*E-mail:* bm2119@columbia.edu